Acta Crystallographica Section D
**Biological Crystallography**
ISSN 0907-4449

# Crystallization and preliminary structural results of catalase from human erythrocytes

**Maria J. Maté,[a] Miguel Ortiz-Lombardía,[a] Alberto Marina[b] and Ignacio Fita[a]***

[a]CID-CSIC, Jordi-Girona 18-26, 08034 Barcelona, Spain, and [b]Instituto de Biomedicina de Valencia (CSIC), C/ Jaume Roig 11, Valencia-46010, Spain

Correspondence e-mail: ifrcri@cid.csic.es

Received 17 December 1998
Accepted 16 February 1999

Catalase (hydrogen peroxide:hydrogen peroxide oxidoreductase, E.C. 1.11.1.6) is present in most aerobic prokaryotic and eukaryotic cells. Despite a large number of studies on catalases, the only mammalian catalase structure available is that from beef liver, in which about 50% of the haem groups are degraded to bile pigments. Three different crystal forms of human erythrocyte catalase were obtained by the hanging-drop vapour-diffusion technique using PEG as precipitant. Monoclinic crystals, with space group $P2_1$ and unit-cell parameters $a$ = 102.9, $b$ = 140.0, $c$ = 173.6 Å and $\beta$ = 103.2°, require NADP(H) in the crystallization solution. Two types of hexagonal packing, with unit-cell parameters of either $a = b$ = 86.9, $c$ = 255.5 Å or $a = b$ = 90.0, $c$ = 521.2 Å, were obtained under identical crystallization conditions in the absence of NADP(H). Only one diffraction data set could be collected: this was obtained from the hexagonal crystals with the smaller $c$ axis using synchrotron radiation, with resolution to 2.65 Å. A molecular-replacement solution, determined using a modified beef-liver catalase model as a search structure, corresponds to space group $P6_422$ and contains a single subunit in the asymmetric unit, with an estimated solvent volume of about 50%. The packing determined suggests how minor rearrangements might allow the transition between both hexagonal crystal forms and provides an explanation for the anisotropic character of the corresponding diffractions.

## 1. Introduction

Catalase (hydrogen peroxide:hydrogen peroxide oxidoreductase, E.C. 1.11.1.6) is present in most aerobic prokaryotic and eukaryotic cells. Catalase decomposes hydrogen peroxide ($H_2O_2$) to water and oxygen either in a two-step catalatic reaction with $H_2O_2$ or in a peroxidatic reaction involving $H_2O_2$ and electron donors such as reduced pyridine nucleotides or ethanol. The catalatic reaction predominates when the $H_2O_2$ concentration is equal to or higher than $10^{-4}$ $M$, while the peroxidatic reaction is the rule in the presence of an acceptable hydrogen donor when the concentration of $H_2O_2$ is below $10^{-4}$ $M$ or when the substrate is an alkyl peroxide (Deisseroth & Dounce, 1970). $H_2O_2$ is a dangerous form of active oxygen owing to its high stability, its diffusion through lipid bilayers and its capacity to form hydroxyl radicals (Halliwell & Gutteridge, 1990; Cadenas, 1989). On the other hand, recent studies describe a role for $H_2O_2$ in signal transduction (Khan & Wilson, 1995; Suzuki *et al.*, 1997).

In mammals, the highest concentrations of catalase are found in the liver and erythrocytes. These contain a number of enzymatic systems catalyzing oxidative degradations which are expected to generate peroxides. In the erythrocyte, both catalase and haemoglobin are shielded from $H_2O_2$ present in the bloodstream by the red-cell membrane. When $H_2O_2$ penetrates this membrane, catalase activity and its ability to decompose $H_2O_2$ appear to be deeply connected to the protection of haemoglobin against oxidation. Catalase was considered to be the enzyme responsible for disposing of all $H_2O_2$ until glutathione peroxidase (GPO) was shown to use glutathione (GSH) to reduce $H_2O_2$ to water (Mills, 1957). The resulting oxidized gluthatione (GSSG) is known to be returned to the reduced state by glutathione reductase using nicotinamide adenine dinucleotide phosphate (NADPH). Cohen & Hochstein (1963) concluded that glutathione peroxidase, linked to the hexose shunt activity, was the major pathway for $H_2O_2$ metabolism in intact erythrocytes. This notion arose from the susceptibility to peroxidative damage of human erythrocytes which had a limited ability to generate NADPH owing to a genetic deficiency in glucose-6-phosphate dehydrogenase (G6PD). Kirkman & Gaetani (1984) demonstrated that mammalian catalase binds NADPH, which in part prevents and reverses the inactivation of the enzyme by its

own substrate. Therefore, both the mechanisms for disposal of $H_2O_2$ are NADPH dependent, thus compromising the interpretation of the observation previously reported. Furthermore, studies comparing normal cells with acatalasemic erythrocytes (Jacobs *et al.*, 1965; Gaetani *et al.*, 1989) and with erythrocytes with inactivated catalase (Gaetani *et al.*, 1994) concluded that catalase eliminates about half the $H_2O_2$ generated in those cells. More recent studies, carried out with a mixture of catalase and GPO in a cell-free system, concluded that catalase accounts for more than 50% of the removal of $H_2O_2$ (Gaetani *et al.*, 1996). A new assay, which allows the determination of GPO and catalase activity at physiological and non-toxic levels of $H_2O_2$ as well as at GSH concentrations normally found in erythrocytes (Mueller *et al.*, 1997*a*), has recently shown that removal of $H_2O_2$ in intact human erythrocytes is almost exclusively accounted for by catalase (Mueller *et al.*, 1997*b*).

Despite a large number of studies on catalases, the only mammalian catalase structure available is that from beef liver (Fita *et al.*, 1986). Amino-acid sequences are well preserved among mammalian catalases, although post-translational modifications can introduce significant differences, which in liver catalases result in about 50% of the haem groups being degraded to bile pigments and a shortened C-terminus (Fita & Rossmann, 1985). The crystallization and preliminary structure determination of a human erythrocyte catalase is reported in this work. Structures determined from these crystals should allow the investigation of intriguing features of catalases such as the haem group alterations, the NADPH binding and its possible correlation with the C-terminus conformation.

## 2. Results and discussion

Samples of human erythrocyte catalase (HEC) from Calbiochem, at initial concentrations of 8 mg ml$^{-1}$ in 50 m*M* TRIS pH 8, were used in extensive crystallization screenings using vapour-diffusion methods. Four different crystal morphologies were obtained (Fig. 1): (*a*) plate-like crystals, (*b*) crystals with poorly defined morphology, (*c*) hexagonal bipyramidal crystals and (*d*) hexagonal needles. The plate-like crystals appeared within 3 d in 16% PEG 10000, 75 m*M* KCl, 100 m*M* Tris pH 9, and required NAPD(H) added to the protein sample solution at ten times the protein concentration. These crystals belong to the monoclinic space group $P2_1$ (unit-cell parameters $a$ = 102.9, $b$ = 140.0, $c$ = 173.6 Å, $\beta$ = 103.2°) and diffracted beyond 3 Å resolution on a Rigaku rotating-anode X-ray source running at 40 kV and 100 mA using a graphite monochromator. A cryo-protectant buffer was not found and the crystals decayed rapidly when exposed to radiation. It has not been possible to reproduce these crystals, so they could not be investigated with synchrotron radiation. The crystals with poorly defined morphologies and the bipyramidal crystals were obtained with 13–16% PEG 10000 and 50–250 m*M* KCl, adding 0.1 *M* of glutaric acid. Both crystal forms, analyzed using synchrotron radiation, showed diffraction symmetry 6/*mmm* and unit-cell parameters $a = b$ = 86.9, $c$ = 255.5 Å and $a = b$ = 90.0, $c$ = 521.2 Å, respectively. The best-looking crystals, with needle-like morphologies, grew to longer than 1 mm and appeared in a few days at 7% PEG 6000, 0.5 *M* NaCl and 100 m*M* Tris pH 9 and also at 10% PEG 3350, 0.25 *M* KCl and 100 m*M* Tris pH 9. Despite their promising appearance, the faces of these crystals were often ridged and no diffraction was obtained from them even when using synchrotron radiation. The critical role played by the NADPH during crystallization of HEC might be related to the heterogeneity arising from partial occupancy of the cofactor. NADPH, with a high affinity for HEC ($K_D < 10^{-8}$ *M*), is expected to remain bound even in those crystals where the cofactor had not been explicitly added. A similar situation had already been found for beef-liver catalase (BLC; Kirkman & Gaetani, 1984).

For the hexagonal crystals with the smaller unit cell, a diffraction data set was collected on beamline X11 at DESY (EMBL Outstation, Hamburg) from a single flash-cooled shapeless crystal, using a cryo-protectant buffer of 30% PEG 10000, 100 m*M* KCl, 100 m*M* Tris pH 9 and 5% ethyleneglycol. These data, processed and scaled with *MOSFLM* (Leslie, 1990) and *SCALA* (Evans, 1997), respectively, gave an overall completeness of 99% to 2.65 Å with 19516 independent reflections and an overall $R_{\rm merge}$ of 7.8% (completeness and $I/\sigma$ in the resolution shell 2.79–2.65 were 99.3% and 1.7, respectively). Systematic absences in the 00*l* reflections suggested the space group to be $P6_222$ (or its enantiomorph $P6_422$). Consideration of the crystal density indicated the most likely presence of only one catalase subunit in the crystal asymmetric unit, which would correspond to a specific volume ($V_m$) of 2.3 Å$^3$ Da$^{-1}$ (Matthews, 1968). Therefore, assuming that the erythrocyte catalase molecule is a

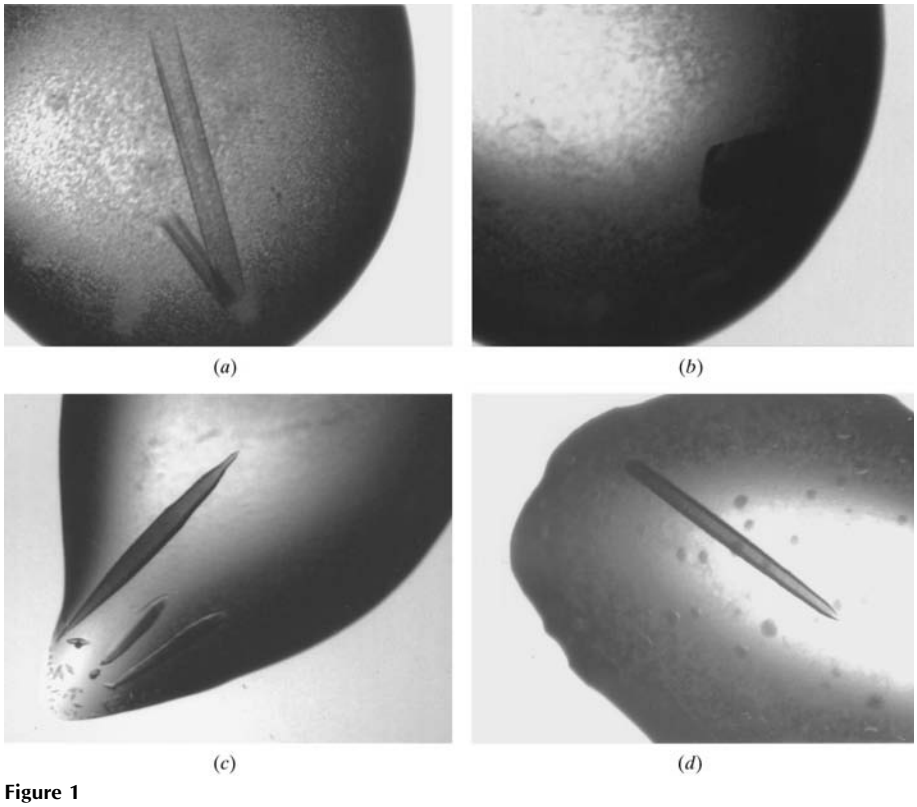


**Figure 1**
Different crystal morphologies obtained from human erythrocyte catalase. (*a*) Plate-like crystals which appeared when NADPH was added to the protein solution. (*b*) Crystals with poorly defined morphology which gave the best diffraction (Fig. 2). (*c*) Crystals with approximately bipyramidal morphology which presented a long *c* axis of 521.2 Å (Fig. 2). (*d*) No diffraction was observed from the needle-like crystals, which grew to longer than 1 mm and often presented ridged faces.

**Table 1**
Summary of the crystals forms obtained, with corresponding crystallization conditions and unit-cell parameters.

In all cases the protein concentration was 8 mg ml$^{-1}$, the precipitant was added to a 1:1 ratio and the volume of the reservoir was 1 ml. All crystals were grown at room temperature.

| Type of crystal | Crystallization conditions | NADPH | Space group | Cell parameters (Å, °) |
|---|---|---|---|---|
| Plate-like | 16% PEG 10000, 75 m*M* KCl, 0.1 *M* Tris pH 9 | Yes | $P2_1$ | $a$ = 102.9, $b$ = 140.0, $c$ = 173.6, $\beta$ = 103.2 |
| Needles | 7% PEG 6000, 0.5 *M* NaCl, 0.1 *M* Tris pH 9 | No | No diffraction | |
| Bipyramidal | 13–16% PEG 10000, 50–250 m*M* KCl, 0.1 *M* Tris pH 9, 0.1 *M* glutaric acid | No | $P6_522$ | $a = b$ = 90.0, $c$ = 521.2 |
| Poorly defined | 13–16% PEG 10000, 50–250 m*M* KCl, 0.1 *M* Tris pH 9, 0.1 *M* glutaric acid | No | $P6_422$ | $a = b$ = 86.9, $c$ = 255.5 |

tetramer with 222 point-group symmetry, the three perpendicular molecular binary axes had to coincide with crystallographic dyad axes. In each of the two possible space groups, two different positions in the asymmetric unit obey this condition. In every position, six molecular orientations, resulting from permutations of the molecular axes had to be considered. A clear solution was determined ($R$ factor of 47.8% and intensities correlation of 48.3% for data to 3.5 Å) by molecular replacement using the program *AMoRe* (Navaza, 1994). The search model used corresponded to a modified BLC subunit in which the N-terminal 74 residues were omitted and a number of other smaller changes were made to allow for the HEC peculiarities. The solution found for space group $P6_422$ with the molecular centre situated in position $(\frac{1}{2}, \frac{1}{2}, \frac{1}{6})$ was among the 24 possibilities referred to previously. The crystal packing obtained does not leave empty spaces large enough to contain another catalase subunit and gives an approximate solvent volume content of 50%.

Strong packing forces would be expected to originate from the large contact areas between the helical C-terminal domains of neighbouring catalase molecules along the sixfold crystal axis. However, only a limited number of interactions appear to stabilize the crystal in the directions perpendicular to the $c$ axis. Thus, optimization of the dominant packing forces might be achieved simply by relaxing the restraint imposed by the coincidence of the molecular dyad and the crystallographic dyad axes parallel to $c$. Retaining all the other symmetry elements would then result in packing according to space group $P6_522$, a maximal non-isomorphic subgroup of $P6_422$ found in the molecular-replacement solution, with the new $c$ axis approximately doubled in length. This observation might explain, at least in part, the presence of the two hexagonal crystal forms in the same crystallization conditions with similar $a$ (and $b$) unit-cell dimensions but values of 255.5 and 521.2 Å, respectively, for the $c$-axis length. The larger unit-cell crystal would contain two catalase subunits in the asymmetric unit with only one of the binary molecular dyad axes coincident with a crystal symmetry. The anisotropic character of the forces stabilizing the two hexagonal packings also appears to be reflected in their diffraction, which attenuates more rapidly in the direction perpendicular to $c^*$ (Fig. 2). In fact, anisotropic scaling performed with *REFMAC* (Murshudov *et al.*, 1997) coincides with values for overall temperature factors along different directions of the reflection data (Hendrickson & Sheriff, 1987), indicating that the diffraction decay is not a peculiar feature of the molecular structure, but mostly a consequence of the anisotropy of the packing.

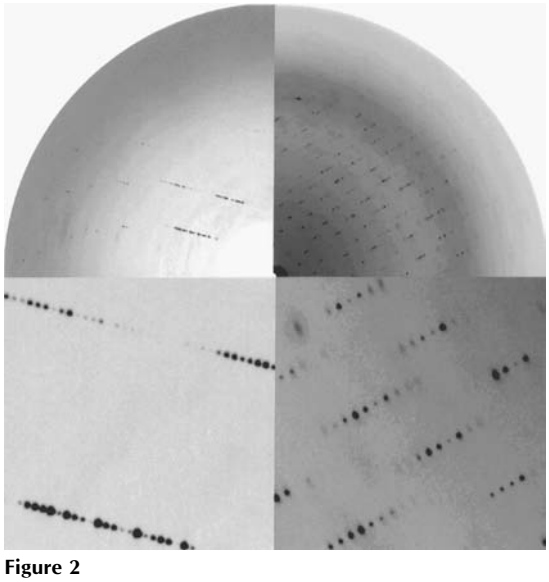

**Figure 2**
Diffraction images from the bipyramidal crystals and from the crystals with poor morphology (left and right sides of the figure, respectively). A long $c$ axis of 521.2 Å can be appreciated in the enlarged left insert. This long $c$ axis is about twice the length of the $c$ axis in the diffraction shown on the right, which clearly extends beyond the detector edge corresponding to a 2.6 Å resolution. For both crystals, diffraction decays more rapidly in the directions perpendicular to the longest axis.

Crystals reported in this work should allow structural characterization of the peculiarities of catalase in erythrocytes, particularly with respect to mammalian liver catalases. The human origin of the catalase analyzed adds specific interest to the accurate determination of the corresponding molecular structures.

Many thanks are due to Pedro M. Alzari for his helpful advice, mainly on molecular replacement. This work was supported by CERBA from Generalitat de Catalunya and by projects PB95-0218 and PM97-0134-CO2-01 from Dirección General de Enseñanza Superior (DGES) of Spain. Data collection at the synchrotron was supported by the Human Capital and Mobility Program of the European Union.

## References

Cadenas, E. (1989). *Annu. Rev. Biochem.* **58**, 79–110.
Cohen, G. & Hochstein, P. (1963). *Biochemistry*, **2**, 1420–1428.
Deisseroth, A. & Dounce, A. L. (1970). *Physiol. Rev.* **50**, 319–374.
Evans, P. R. (1997). *Jnt CCP4/ESF–EACBM Newslett.* **33**, 22–24.
Fita, I. & Rossmann, M. G. (1985). *Proc. Natl Acad. Sci. USA*, **82**, 1604–1608.
Fita, I., Silva, A. M., Murthy, M. R. N. & Rossmann, M. G. (1986). *Acta Cryst.* B**42**, 497–515.
Gaetani, G. F., Ferraris, A. M., Rolfo, M., Mangerini, R., Arena, S. & Kirkman, H. N. (1996). *Blood*, **87**, 1595–1599.
Gaetani, G. F., Galiano, S., Canepa, L., Ferraris, A. M. & Kirkman, H. N. (1989). *Blood*, **73**, 334–339.
Gaetani, G. F., Kirkman, H. N., Mangerini, R. & Ferraris, A. M. (1994). *Blood*, **84**, 325–330.
Halliwell, B. & Gutteridge, J. M. C. (1990). *Methods Enzymol.* **186**, 1–90.
Hendrickson, W. A. & Sheriff, S. (1987). *Acta Cryst.* A**43**, 121–125.
Jacobs, H. S., Ingbar, S. H. & Jandl, J. H. (1965). *J. Clin. Invest.* **44**, 1187–1198.
Khan, A. U. & Wilson, T. (1995). *Chem. Biol.* **2**, 437–445.
Kirkman, H. N. & Gaetani, G. F. (1984). *Proc. Natl Acad. Sci. USA*, **81**, 4343–4347.
Leslie, A. G. W. (1990). *Crystallographic Computing.* Oxford University Press.
Matthews, B. W. (1968). *J. Mol. Biol.* **33**, 491–497.
Mills, G. C. (1957). *J. Biol. Chem.* **229**, 189-
Mueller, S., Riedel, H. D. & Stremmel, W. (1997*a*). *Anal. Biochem.* **245**, 55–60.
Mueller, S., Riedel, H. D. & Stremmel, W. (1997*b*). *Blood*, **90**, 4973–4978.
Murshudov, G. N., Vagin, A. A. & Dodson, E. J. (1997). *Acta Cryst.* D**53**, 240–255.
Navaza, J. (1994). *Acta Cryst.* A**50**, 157–163.
Suzuki, Y. J., Forman, H. J. & Sevanian, A. (1997). *Free Radic. Biol. Med.* **22**, 269–285.